Acyclic Cucurbit[n]uril Molecular Containers Selectively Solubilize Single-Walled Carbon Nanotubes in Water

ARTICLE *in* JOURNAL OF THE AMERICAN CHEMICAL SOCIETY · APRIL 2012

Impact Factor: 12.11 · DOI: 10.1021/ja301462e · Source: PubMed

JACS
JOURNAL OF THE AMERICAN CHEMICAL SOCIETY

Communication

pubs.acs.org/JACS

Acyclic Cucurbit[*n*]uril Molecular Containers Selectively Solubilize Single-Walled Carbon Nanotubes in Water

Cai Shen,[#] Da Ma,[‡] Brendan Meany, Lyle Isaacs,* and YuHuang Wang*

Department of Chemistry and Biochemistry, University of Maryland, College Park, Maryland, United States

Supporting Information

ABSTRACT: Making single-walled carbon nanotubes (SWNTs) soluble in water is a challenging first step to use their remarkable electronic and optical properties in a variety of applications. We report that acyclic cucurbit[*n*]-uril molecular containers **1** and **2** selectively solubilize small-diameter and low chiral angle SWNTs. The selectivity is tunable by increasing the concentration of the molecular containers or by adjusting the ionic strength of the solution. Even at a concentration 1000 times lower than typically required for surfactants, the molecular containers render SWNTs soluble in water. Molecular mechanics simulations suggest that these C-shaped acyclic molecules complex the SWNTs such that a large portion of nanotube sidewalls are exposed to the external environment. These "naked" nanotubes fluoresce upon patching the exposed surface with sodium dodecylbenzene sulfonate.

Single-walled carbon nanotubes (SWNTs) are insoluble in water and virtually all other conventional solvents, but the electronic and optical properties that make SWNTs desirable electronic materials and biosensors are observed only in their individually dispersed states.[1] For this reason, enormous efforts have been devoted over the past decade to addressing this insolubility problem.[2−9] A successful common approach involves the use of a surfactant, such as sodium dodecyl sulfate (SDS), sodium dodecylbenzene sulfonate (SDBS), Triton X-100, and sodium cholate, to encapsulate the nanotube in micelles. Other approaches include wrapping the nanotube with synthetic polymers, DNA, or proteins to improve solubility and dispersion of the nanotubes.[3−6] However, the need for excess surfactants and the labile nature of the micelle structures often pose limitations to their applications.

Another major challenge in using SWNTs is their broad structural distribution. Furthermore, each different structural type of SWNT may exhibit significant differences in its chemical and physical properties. Accordingly, there has been great interest in the search for complexing agents that selectively solubilize SWNTs on the basis of their diameter and their chirality. Some successes have been achieved with specific DNA sequences that selectively wrap around SWNTs according to diameter and chirality,[7] polyfluorenes that show the ability to discriminate between nanotube species in terms of either diameter or chiral angle,[10] chiral diporphyrin molecules that possess different binding affinities for left- and right-handed helical nanotube isomers,[11] and flavin mononucleotide that preferentially binds (8,6)-SWNTs through concentric interactions between the two.[12] These molecular systems greatly deepen our understanding of the intermolecular interactions and properties of SWNTs in solution, which can potentially lead to the design of molecules for structure-specific separation of SWNTs on a large scale. However, there is a great need for additional systems that display selective intermolecular interactions with specific classes of SWNTs for use in the separation and solubilization of SWNTs.

The cucurbit[*n*]uril family of molecular containers (CB[*n*], *n* = 5, 6, 7, 8, 10) is attracting significant interest because of their ability to bind to hydrophobic and cationic species in aqueous solution.[13−16] Recently, we reported the synthesis of two highly soluble acyclic cucurbituril congeners (**1** and **2**) with the ability

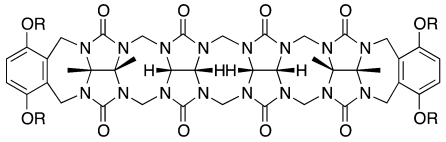

1 R = $(CH_2)_3SO_3Na$

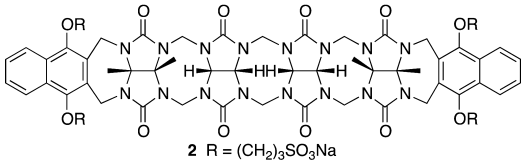

2 R = $(CH_2)_3SO_3Na$

to solubilize a variety of hydrophobic pharmaceutical agents.[17] In this paper, we show that **1** and **2** solubilize individual SWNTs in water even at a concentration 100−1000 times lower than typically required for surfactants or previous molecular systems.[10,11] The dispersion process is diameter dependent and exhibits selectivity toward low chiral angle structures, an important capability that is complementary to existing methods.[10,11] The structural selectivity is tunable based on the structure of the acyclic CB[*n*] receptor used and the concentration of added salt.

Molecular containers **1** and **2** are composed of a central glycoluril tetramer unit that by virtue of the fused polycyclic ring system is preorganized into a C-shape, which is capped by two substituted aromatic rings that are terminated in sodium sulfonate groups.[17] We expected that the aromatic walls of **1** and **2** would allow them to form complexes with SWNTs driven by $\pi-\pi$ interactions, whereas the sulfonate groups would render **1**, **2**, and their SWNT complexes soluble in water.

Received: February 13, 2012
Published: April 18, 2012

   dx.doi.org/10.1021/ja301462e | *J. Am. Chem. Soc.* 2012, 134, 7254−7257

Furthermore, by virtue of their acyclic nature, compounds **1** and **2** are able to expand the size of their cavities by conformational changes at the CH_2 bridges of their polycyclic backbone in much the same way as a hand flexes.[17,18] Such conformational flexibility allows **1** and **2** to adapt their shape to interact maximally with SWNTs. Compounds **1** and **2** are acyclic members of the cucurbit[*n*]uril family of molecular containers and were therefore expected to retain the excellent recognition properties of this class of molecules toward cationic species in water.[13,15−18]

Figure 1 shows a molecular mechanics model of an (8,3)-SWNT encapsulated by **1** in water. The optimized structure

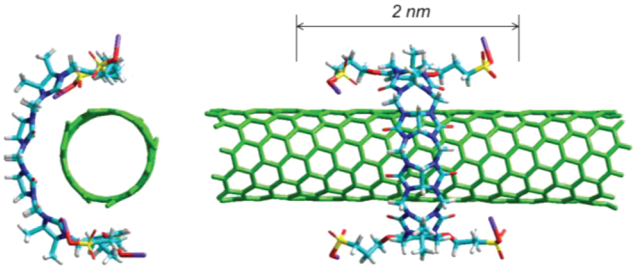

Figure 1. Molecular mechanics model of the complex between an (8,3)-nanotube and container **1**. The geometry was optimized with HyperChem 8 applying the MM+ force field. The nanotube is 3.5 nm long, and both ends are terminated by hydrogen atoms. Solvation is accounted for by applying a 3 nm × 3 nm × 4 nm periodic box of water molecules. For clarity, the water molecules are not shown.

shows that the C-shaped molecule attaches to the nanotube like a clip, leaving portions of the nanotube exposed to the local environment. The model suggests that a single molecule of **1** covers approximately a 2 nm length along the SWNT. From molecular modeling, we know that a 2 nm length of an (8,3)-SWNT contains 190 C-atoms weighing 2282 g mol^{-1}, which is comparable to the molecular weight of **1** (1541.4 g mol^{-1}). This simple calculation suggests that the amount of **1** required to fully cover the SWNT occurs at a 0.7:1 wt:wt ratio. Owing to the high water solubility of **1** (~346 mM),[17] this molecular container readily renders small-diameter SWNTs soluble in water (Figure 2a). Because these molecular containers are not traditional surfactants, they do not exhibit a critical micelle concentration over the range of experimental conditions employed. There is, therefore, no need to use an excess amount of **1** to stabilize the SWNT dispersion in aqueous solution. Even at 0.001 wt%, a concentration 1000 times lower than that required of commonly used surfactants,[19,20] **1** can disperse SWNTs to a concentration of 12.5 mg/L (Figure 2). To further understand this behavior, we performed titration experiments to quantify the amount of solubilized SWNTs as a function of the initial SWNT load and the starting concentrations of **1**. At a fixed concentration of **1** (0.001 wt %), individually dispersed SWNTs solutions of 4.8, 6.8, and 12.5 mg/L were obtained from starting suspensions of 20, 40, and 80 mg/L of HiPco SWNTs in D_2O, respectively. When the SWNT load was increased to 120 mg/L, the absorption of both **1** and carbon nanotubes surprisingly decreased (Figure 2a). This observation was very reproducible. Similarly, at a fixed SWNT load of 20 mg/L, the final nanotube concentration decreases as the concentration of **1** increases from 0.001 to 0.4 wt% (Figure S1). This titration experiment shows that **1** is capable of stabilizing the SWNT even at a concentration that is

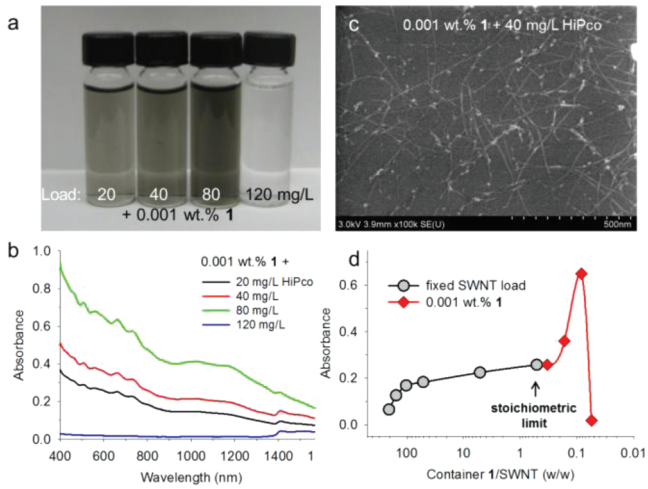

Figure 2. Compound **1** solubilizes SWNTs below the stoichiometric limit. (a) Photograph of **1**·SWNTs dispersions prepared from increasing initial nanotube load in 0.001 wt% solutions of **1**. (b) Visible−NIR absorption spectra of the corresponding dispersions. (c) Representative scanning electron microscopy image of the resulting **1**·SWNTs on a silicon substrate. (d) Optical absorbance of individually dispersed SWNTs at 600 nm versus the weight ratio of **1** to SWNT load. As the relative load of **1** decreases, the concentration of individually dispersed SWNTs steadily increases until the stoichiometric limit. At ratios well below the stoichiometric limit, a maximum is reached, followed by a sharp decrease. The stoichiometric limit, as revealed by the molecular mechanics model, corresponds to one molecule of **1** approximately every 2 nm length of SWNT.

well below the 0.7:1 ratio of a fully covered **1**·SWNT structure. Because of the low concentration of **1**, **1**·SWNT structures could be cleanly deposited on silicon substrates by direct drying of a droplet (Figures 2c and S2). However, due to drying-induced aggregation, it is difficult to prevent nanotubes from bundling. More conclusive evidence regarding their dispersion states in solutions was obtained from spectroscopic studies.

UV−vis−NIR absorption spectra of the **1**·SWNTs solutions are nearly featureless. However, upon adding SDBS and shaking the solution by hand, the distinct van Hove absorption peaks that are characteristic of individually dispersed SWNTs[21] were recovered (Figures 3a and S3). Consistently, SWNTs solubilized with **1** initially did not fluoresce; however, strong fluorescence was observed upon the addition of SDBS (Figure 3b). Both fluorescence and van Hove absorption are characteristic of individually dispersed SWNTs. Interestingly, the nanotubes must have already become debundled by **1** since no sonication was required to recover the optical features; rather, gentle shaking by hand was sufficient. This behavior suggests the **1**·SWNTs were not strongly bundled but loosely associated individual nanotubes in water. We believe that the added SDBS molecules patch the exposed nanotube surface to recover the fluorescence and optical absorption by insulating the SWNT from the environment and interactions with other nanotubes. This explanation is consistent with previous observation of enhanced fluorescence as the nanotube surface is more densely covered with an aliphatic analogue of flavin mononucleotide.[22] The observed fluorescence turn-on effect may be useful in biomolecular sensing[23] and will be further explored in future studies.

Intriguingly, excitation−emission fluorescence maps suggest that the container **1** selectively interacts with smaller diameter and low chiral angle SWNTs (Figure 4). Compared to SDBS

dx.doi.org/10.1021/ja301462e | *J. Am. Chem. Soc.* 2012, 134, 7254−7257

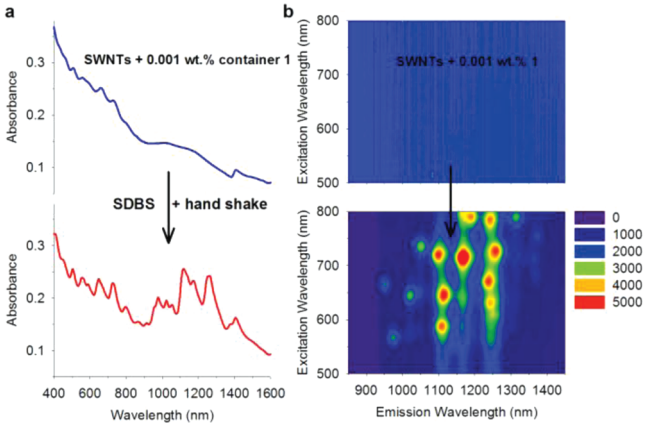

Figure 3. Turn-on of optical properties upon addition of SDBS. The optical absorption (a) and fluorescence (b) that are characteristic of individually dispersed SWNTs were turned on upon addition of SDBS (to a concentration of 1.0 wt%). Shown is the case of 20 mg/L nanotube load in 0.001 wt% **1**, but this phenomenon is general to all experimental conditions investigated in this work.

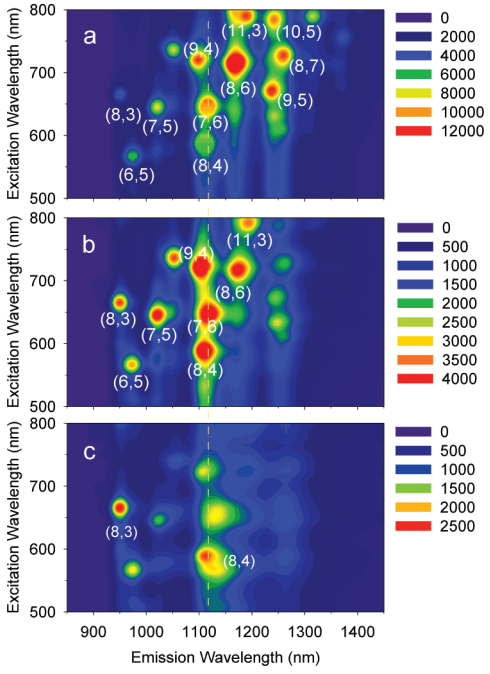

Figure 4. Excitation–emission fluorescence maps show evidence of selective enrichment of smaller diameter SWNTs in aqueous solutions by container molecules. Shown are solutions prepared from an initial load of 20 mg/L HiPco SWNTs and (a) 1 wt% SDBS, (b) 0.1 wt% **1**, and (c) 0.1 wt% **2**. Compared to SDBS control, **1** favors smaller diameter SWNTs. The structural selectivity is further evidenced in **2**.

(Figure 4a), **1** and **2** (Figure 4b,c) show a clear tendency of much higher fluorescence intensities for smaller diameter nanotubes. Interestingly, the fluorescence intensity of SWNTs systematically decreases as the concentration of **1** increases from 0.001 to 0.4 wt% (Figure S4). For the 0.4 wt% solution of **1**, strong emission peaks correspond to small diameter SWNTs: (8,3), (8,4), and (9,4) with diameters of 7.8, 8.4, and 9.2 Å, respectively. The (8,3)-SWNT accounts for 15.8% of the fluorescence intensity of the 0.4 wt% **1**·SWNTs solution, more than 3 times higher than that in the 0.001 wt% **1** sample. On the other hand, the total amount of dispersed large-diameter (d > 0.95 nm) SWNTs (8,6), (8,7), (9,5), and (10,5) decreases by 45% as the concentration of **1** increases (Figures S5). There is also a selectivity toward low chiral angle SWNTs, demonstrated by a stronger emission signal for (9,4) compared with (7,6), even though their diameters are similar (Figure S5). We also observed changes in the UV–vis–NIR absorption spectra which are consistent with the selectivity patterns described above. However, the lower inherent sensitivity of the optical absorption spectra to differences in SWNT structure and the significant background signal due to other carbonaceous byproducts make the fluorescence experiments described above more authoritative.

The observed concentration-dependent diameter selectivity can be explained by salt effects. We found that addition of 2.5 mM NaCl made the SWNT fluorescence map of 0.001 wt% **1** solution similar to that of the 0.1 wt% **1** solution, which contains ~2.6 mM Na^+ (see Figure S6). As the NaCl concentration is increased from 0 to 3.5 mM, there is a systematic decrease of the SWNT fluorescence intensity toward smaller diameter SWNTs, as shown in Figures S5 and S7. For small-diameter, low chiral angle species such as (8,3) and (8,4), the populations are similarly enhanced by increasing the concentration of either **1** or the salt. For large-diameter species (8,6), (9,5), and (10,5), the populations are reduced. However, small-diameter, high chiral angle species (6,5) and (7,6) are not affected. These trends are corroborated by the corresponding visible–NIR absorption spectra (Figure S8). The salt effect was enhanced with a divalent salt solution. A concentration of 0.05 mM $CaCl_2$, compared to 2.5 mM NaCl, already shifts the selectivity toward small-diameter SWNTs.

We rationalize the observed preference of **1** for smaller diameter SWNTs at higher salt concentration based on the well-known metal ion binding properties of CB[n] compounds. The presence of metal cations rigidifies the C-shape of **1** by bridging adjacent C=O groups, which results in higher curvature and a preference for smaller SWNTs. Conversely, in the absence of metal cations, **1** is better able to expand its cavity to accommodate the larger diameter SWNTs. This is consistent with previous observations by us and others that increasing the concentration of metal cations reduces the affinity of the acyclic cucurbit[n]uril congener toward guest molecules due to binding competition at the ureidyl C=O portals.[18,24,25] The preference for low chiral angle SWNTs can be explained by the calculated geometry of the **1**·SWNT complex (Figure 1). For low chiral angle SWNTs, the π–π stacking interactions are stronger due to the matched orientation of the terminating aromatic motifs of **1**, whereas for high chiral angle tubes, the π–π interactions are weaker. As a test of the importance of π–π interactions toward selective solubilization, we decided to investigate the interaction of **2** with SWNTs. The strength of the π–π interactions between the SWNTs and the acyclic CB[n]-type receptor **2** would be expected to increase (relative to **1**) because of the larger π-surface area of the naphthalene walls of **2**. Satisfyingly, as shown in Figure 4c, acyclic CB[n]-type container **2** shows similar optical turn-on effects (Figure S10) and a clear selectivity toward low chiral angle, small-diameter (8,3) and (8,4) SWNTs at much lower (salt) concentrations.

In summary, we have shown that acyclic cucurbit[n]uril-type molecular containers **1** and **2** are able to solubilize SWNTs at concentrations (0.001 wt%) that are 1000-fold lower than used in standard SDBS solubilization. The C-shaped molecular containers clip-on to SWNTs by a combination of π–π

dx.doi.org/10.1021/ja301462e | J. Am. Chem. Soc. 2012, 134, 7254–7257

interactions and the hydrophobic effect, and render nanotubes solubilized in water due to the presence of the sulfonate groups on **1** and **2**. Compounds **1** and **2** display a selectivity toward small-diameter and low chirality SWNTs due to the inherent curvature of **1** and **2** and the nature of the $\pi-\pi$ interactions between the aromatic walls of the molecular containers and the SWNTs. The presence of metal ions (e.g., Na^+ or Ca^{2+}) enhances the selectivity for small-diameter, low chiral angle tubes by binding to the ureidyl C=O portals of **1** and **2**, thereby rigidifying their structures and making them less able to flex their methylene-bridged glycoluril oligomer backbones to accommodate larger SWNTs. The implications of the research presented are manifold. For example, by tailoring the nature of the aromatic walls of the acyclic CB[*n*]-type containers, it should be possible to tune the selectivity toward specific classes (e.g., diameter, chirality) of SWNTs. The ability of **1** and **2** to solubilize SWNTs at low concentrations while leaving the nanotube surface exposed enables the preparation of hybrids with biomolecular receptors, which are expected to combine the advantageous optical properties of the SWNTs with the molecular recognition ability of the biomolecules.

■ ASSOCIATED CONTENT

Ⓢ Supporting Information

Materials, methods, modeling, and Figures S1−11. This material is available free of charge via the Internet at http://pubs.acs.org.

■ AUTHOR INFORMATION

Corresponding Author

yhw@umd.edu; lisaacs@umd.edu

Present Addresses

[#]Interdisciplinary Nanoscience Center, Aarhus University, [‡]Denmark

[‡]Department of Chemistry, University of North Carolina, Chapel Hill, North Carolina

Notes

The authors declare no competing financial interest.

■ ACKNOWLEDGMENTS

Y.W. gratefully acknowledges support from the Office of Naval Research (N000141110465), National Science Foundation (CAREER CHE-1055514), and the University of Maryland. L.I. and D.M. thank the National Science Foundation (CHE-1110911) for financial support.

■ REFERENCES

(1) O'Connell, M. J.; Bachilo, S. M.; Huffman, C. B.; Moore, V. C.; Strano, M. S.; Haroz, E. H.; Rialon, K. L.; Boul, P. J.; Noon, W. H.; Kittrell, C.; Ma, J.; Hauge, R. H.; Weisman, R. B.; Smalley, R. E. *Science* **2002**, *297*, 593.

(2) O'Connell, M.; Boul, P.; Ericson, L. M.; Huffman, C.; Wang, Y. H.; Haroz, E.; Ausman, K. D.; Smalley, R. E. *Chem. Phys. Lett.* **2001**, *342*, 265.

(3) Backes, C.; Schmidt, C. D.; Rosenlehner, K.; Hauke, F.; Coleman, J. N.; Hirsch, A. *Adv. Mater.* **2010**, *22*, 788.

(4) Lin, S. C.; Blankschtein, D. *J. Phys. Chem. B* **2010**, *114*, 15616.

(5) Komatsu, N. *J. Inclusion Phenom. Macrocyclic Chem.* **2008**, *61*, 195.

(6) Star, A.; Stoddart, J. F.; Steuerman, D.; Diehl, M.; Boukai, A.; Wong, E. W.; Yang, X.; Chung, S.-W.; Choi, H.; Heath, J. R. *Angew. Chem., Int. Ed.* **2001**, *40*, 1721.

(7) Zheng, M.; Jagota, A.; Semke, E. D.; Diner, B. A.; Mclean, R. S.; Lustig, S. R.; Richardson, R. E.; Tassi, N. G. *Nat. Mater.* **2003**, *2*, 338.

(8) Brozena, A. H.; Moskowitz, J.; Shao, B.; Deng, S.; Liao, H.; Gaskell, K. J.; Wang, Y. *J. Am. Chem. Soc.* **2010**, *132*, 3932.

(9) Deng, S.; Zhang, Y.; Brozena, A. H.; Mayes, M. L.; Banerjee, P.; Chiou, W. A.; Rubloff, G. W.; Schatz, G. C.; Wang, Y. *Nat. Commun.* **2011**, *2*, 382.

(10) Nish, A.; Hwang, J.-Y.; Doig, J.; Nicholas, R. J. *Nat. Nanotechnol.* **2007**, *2*, 640.

(11) Peng, X.; Komatsu, N.; Bhattacharya, S.; Shimawaki, T.; Aonuma, S.; Kimura, T.; Osuka, A. *Nat. Nanotechnol.* **2007**, *2*, 361.

(12) Ju, S. Y.; Doll, J.; Sharma, I.; Papadimitrakopoulos, F. *Nat. Nanotechnol.* **2008**, *3*, 356.

(13) Nau, W. M.; Florea, M.; Assaf, K. I. *Isr. J. Chem.* **2011**, *51*, 559.

(14) Isaacs, L. *Chem. Commun.* **2009**, 619.

(15) Lee, J. W.; Samal, S.; Selvapalam, N.; Kim, H. J.; Kim, K. *Acc. Chem. Res.* **2003**, *36*, 621.

(16) Ko, Y. H.; Kim, E.; Hwang, I.; Kim, K. *Chem. Commun.* **2007**, 1305.

(17) Ma, D.; Hettiarachchi, G.; Nguyen, D.; Zhang, B.; Wittenberg, J. B.; Zavalij, P. Y.; Briken, V.; Isaacs, L. *Nat. Chem.* **2012**, DOI: 10.1038/nchem.1326.

(18) Ma, D.; Zavalij, P. Y.; Isaacs, L. *J. Org. Chem.* **2010**, *75*, 4786.

(19) Bales, B. L. *J. Phys. Chem. B* **2001**, *105*, 6798.

(20) Niyogi, S.; Boukhalfa, S.; Chikkannanavar, S. B.; McDonald, T. J.; Heben, M. J.; Doorn, S. K. *J. Am. Chem. Soc.* **2007**, *129*, 1898.

(21) Weisman, R. B.; Bachilo, S. M. *Nano Lett.* **2003**, *3*, 1235.

(22) Ju, S.-Y.; Kopcha, W. P.; Papadimitrakopoulos, F. *Science* **2009**, *323*, 1319.

(23) Satishkumar, B. C.; Brown, L. O.; Gao, Y.; Wang, C. C.; Wang, H. L.; Doorn, S. K. *Nat. Nanotechnol.* **2007**, *2*, 560.

(24) Marquez, C.; Hudgins, R. R.; Nau, W. M. *J. Am. Chem. Soc.* **2004**, *126*, 5806.

(25) Burnett, C. A.; Witt, D.; Fettinger, J. C.; Isaacs, L. *J. Org. Chem.* **2003**, *68*, 6184.